

## X-ray Absorption Spectra of the Oxidized and Reduced Forms of C112D Azurin from *Pseudomonas aeruginosa*

Serena DeBeer,<sup>†</sup> Cynthia N. Kiser,<sup>‡</sup> Gary A. Mines,<sup>‡</sup> John H. Richards,<sup>‡</sup> Harry B. Gray,<sup>\*,‡</sup> Edward I. Solomon,<sup>\*,†</sup> Britt Hedman,<sup>\*,§</sup> and Keith O. Hodgson<sup>\*,†,§</sup>

Department of Chemistry, Stanford University, Stanford, California 94305, Beckman Institute, California Institute of Technology, Pasadena, California 91125, and Stanford Synchrotron Radiation Laboratory, Stanford, California 94309

Received April 23, 1998

The oxidized and reduced forms of a mutant of *Pseudomonas aeruginosa* azurin, in which the Cys112 has been replaced by an aspartate, have been studied by X-ray absorption spectroscopy. It is well established that the characteristic ~600 nm absorption feature of blue copper proteins is due to the S(Cys112)  $3p\pi \rightarrow \text{Cu } 3d_{x^2-y^2}$  charge-transfer transition. While other mutagenesis studies have involved the creation of an artificial blue copper site, the present work involves a mutant in which the native blue copper site has been destroyed, thus serving as a direct probe of the importance of the copper–thiolate bond to the spectroscopy, active site structure, and electron-transfer function of azurin. Of particular interest is the dramatic decrease in electron-transfer rates, both electron self-exchange ( $k_{\text{ese}} \approx 10^5 \text{ M}^{-1} \text{ s}^{-1}$  wild-type azurin vs  $k_{\text{ese}} \approx 20 \text{ M}^{-1} \text{ s}^{-1}$  C112D azurin) and intramolecular electron transfer to ruthenium-labeled sites ( $k_{\text{et}} \approx 10^6 \text{ s}^{-1}$  wild-type azurin vs  $k_{\text{et}} \leq 10^3 \text{ s}^{-1}$  C112D azurin), which is observed in the mutant. These changes may be a reflection of significant differences in electronic coupling into the protein matrix ( $H_{\text{AB}}$ ) and/or in the reorganization energy ( $\lambda$ ). These effects can be probed by the use of Cu K-edge X-ray absorption spectroscopy, the results of which indicate both a decrease in the covalency of the active site and an expansion of ~0.2 Å in the Cu coordination sphere trigonal plane upon reduction of the C112D mutant.

### Introduction

The active sites of oxidized blue copper proteins are characterized by unique spectral features compared to those of normal tetragonal Cu(II) complexes.<sup>1–7</sup> The defining features are an intense absorption band centered at ~600 nm ( $\epsilon > 2000 \text{ M}^{-1} \text{ cm}^{-1}$ ), an unusually small parallel hyperfine splitting ( $60 \times 10^{-4} \text{ cm}^{-1}$ ) in the EPR spectrum, and a high reduction potential ( $E^\circ > 150 \text{ mV}$  vs NHE). Development of a detailed understanding of these features and their use as a probe of protein function have been the goals of many experimental and theoretical studies. Mutagenesis experiments are one means by which insight can be gained into the relationship between structure and function in these electron-transfer proteins. By selective substitution of a single amino acid residue, the importance of that residue can be assessed. *Pseudomonas*

*aeruginosa* azurin is particularly well suited to such studies, since it contains only a single copper ion and no cofactors, making it one of the simplest of the blue copper proteins.

The active site of azurin consists of a copper atom coordinated to the nitrogen atoms of two histidine residues (His46 and His117), a cysteine sulfur (Cys112), and a methionine sulfur (Met121). For blue copper proteins, the Cu–N bond lengths are typically in the range 1.9–2.1 Å. The Cu–S (Met121) bond is unusually long (~2.7–3.1 Å) relative to normal Cu–S bond distances (~2.3 Å), while the Cu–S (Cys) bond is significantly shorter (~2.1 Å) than those of normal copper systems.<sup>5</sup> It is this short cysteine–thiolate bond that has been shown to be responsible for many of the unique spectral features of blue copper proteins. Polarized absorption and low-temperature magnetic circular dichroism (MCD) studies in combination with self-consistent X $\alpha$ -scattered wave (X $\alpha$ ) calculations have definitively established that the intense ~600 nm absorption feature is a S(Cys112)  $3p\pi \rightarrow \text{Cu } 3d_{x^2-y^2}$  charge-transfer transition.<sup>8,9</sup> S K-edge X-ray absorption spectroscopy (XAS) edge studies have shown a high degree of covalency in the copper–thiolate bond, which is reflected in the small parallel hyperfine splitting in the EPR spectrum.<sup>10</sup> In addition, the active site cysteine ligand has been proposed to provide strong electronic coupling between the protein and the copper center

\* To whom correspondence should be addressed.

<sup>†</sup> Stanford University.

<sup>‡</sup> California Institute of Technology.

<sup>§</sup> Stanford Synchrotron Radiation Laboratory.

- (1) Groenveld, C. M.; Canters, G. W. *Eur. J. Biochem.* **1985**, *153*, 559–564.
- (2) Mizoguchi, T. J.; Ph.D. Dissertation, California Institute of Technology, Pasadena, CA, 1996.
- (3) Langen, R.; Chang, I. J.; Germanas, J. P.; Richards, J. H.; Winkler, J. R.; Gray, H. B. *Science* **1995**, *268*, 1733–1735.
- (4) Regan, J. J.; DiBilio, A. J.; Langen, R.; Skov, L. K.; Winkler, J. R.; Gray, H. B.; Onuchic, J. N. *Chem. Biol.* **1995**, *2*, 489–496.
- (5) Adman, E. T. *Metalloproteins: Structural Aspects*; Anfinsen, C. B., Edsall, J. T., Eisenberg, D. S., Eds.; Academic Press: 1991; Vol. 42, pp 145–192.
- (6) Gray, H. B.; Solomon, E. I. *Copper Proteins*; Spiro, T. G., Ed.; Wiley: New York, 1980; pp 1–39.
- (7) Solomon, E. I.; Penfield, K. W.; Wilcox, D. E. *Structure and Bonding*; Hemmerich, P., Ed.; Springer-Verlag: New York, 1983; pp 1–57.

(8) Gewirth, A. A.; Solomon, E. I. *J. Am. Chem. Soc.* **1988**, *110*, 3811–3819.

(9) Penfield, K. W.; Gewirth, A. A.; Solomon, E. I. *J. Am. Chem. Soc.* **1985**, *107*, 7, 4519–4529.

(10) Shadle, S. E.; Penner-Hahn, J. E.; Schugar, H. J.; Hedman, B.; Hodgson, K. O.; Solomon, E. I. *J. Am. Chem. Soc.* **1993**, *115*, 767–776.

with respect to electron transfer.<sup>3,4,11–13</sup> It is interesting to note that mutants involving substitution at the active site sulfur methionine<sup>1,14–16</sup> or one of the active site histidines still exhibit spectra which are dominated by the characteristic  $\sim 600$  nm absorption band.<sup>14–19</sup> This demonstrates that these ligands are not strictly required for maintaining the blue copper site, thereby reinforcing the essential role played by Cys112.

Mizoguchi has expressed and characterized a mutant form of *P. aeruginosa* azurin in which the Cys112 has been replaced by an aspartate.<sup>2</sup> Although other mutagenesis experiments have involved the creation of an artificial blue copper site, Mizoguchi's mutant is one in which the native blue copper site has been destroyed. Its properties are consistent with the importance of the copper–thiolate bond to the spectroscopy, active site structure, and electron-transfer function of azurin. The oxidized form of this C112D mutant has spectral properties that are characteristic of a normal tetragonal Cu(II) complex; a larger hyperfine coupling constant in the EPR spectrum ( $A_{\parallel} = 152 \times 10^{-4} \text{ cm}^{-1}$ ), a lower redox potential ( $E^{\circ} = 180 \text{ mV}$  at  $\text{pH} = 7.0$  vs  $E^{\circ} = 308 \text{ mV}$  at  $\text{pH} = 7.0$  for wild-type (WT) azurin), and the absence of an absorption band at  $\sim 600 \text{ nm}$ .<sup>2</sup> In addition, C112D azurin exhibits a dramatic decrease in electron-transfer rates, both electron self-exchange ( $k_{\text{ese}} \approx 10^5 \text{ M}^{-1} \text{ s}^{-1}$  wild-type azurin<sup>1</sup> vs  $k_{\text{ese}} \approx 20 \text{ M}^{-1} \text{ s}^{-1}$  C112D azurin<sup>2</sup>) and intramolecular electron transfer to ruthenium-labeled sites ( $k_{\text{et}} \approx 10^6 \text{ s}^{-1}$  wild-type azurin<sup>3,4</sup> vs  $k_{\text{et}} \leq 10^3 \text{ s}^{-1}$  C112D azurin<sup>2</sup>). These changes may be a reflection of significant differences in electronic coupling into the protein matrix ( $H_{\text{AB}}$ ) and/or in the reorganization energy ( $\lambda$ ).

The electronic coupling matrix element is affected by the covalency of metal–ligand bonds and by the secondary and tertiary structure of the protein. The crystal structure of oxidized C112D azurin indicates that the overall structure is very similar to that of WT azurin.<sup>20</sup> Hence, the coupling provided by the  $\beta$ -sheet structure of azurin is most likely preserved, and it is reasonable to assume that whatever change has occurred in electronic coupling is due to a decrease in covalency at the active site.

The decrease in electron-transfer rates may also be attributed to an increase in  $\lambda$ . A change in the active site structure on going from the oxidized to the reduced form will contribute to the inner sphere reorganization energy and thus provide an additional Franck–Condon barrier to electron transfer. Crystallographic analyses of both the oxidized and reduced forms of WT azurin from *Alcaligenes denitrificans* refined to 1.8 and 1.9 Å resolution, respectively,<sup>21,22</sup> show that the geometry and metrical details remain essentially the same upon reduction. A slight expansion of the copper site is observed for all bond

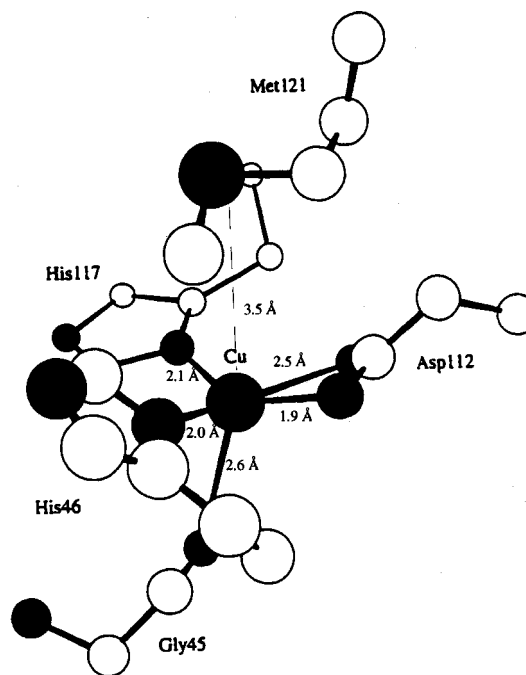


**Figure 1.** Active site of oxidized C112D azurin from *P. aeruginosa* as determined by X-ray crystallographic analysis (adapted from ref 2).

distances, including the axial methionine and the carbonyl oxygen, increasing by 0.05–0.1 Å. It is quite possible, however, that these distance changes are smaller than the error limits of crystallographic refinement at this resolution.<sup>23</sup> The limited distortion upon reduction indicates a small reorganization energy, and thus a low Franck–Condon barrier to electron transfer. It is thus important to have an understanding of the geometric change which occurs upon reduction of this mutant.

The crystal structure of oxidized C112D azurin reveals that there are two crystallographically independent azurin molecules in the asymmetric unit.<sup>20</sup> The nearly identical azurin molecules have a maximum deviation in distance of 0.035 Å at a crystal structure resolution of 2.4 Å. The averaged results show a distorted square pyramidal active site structure in which the copper atom is coordinated by both carboxylate oxygens of Asp112 at distances of 2.5 and 1.9 Å and by the nitrogens of His46 and His117 at distances of 2.0 and 2.1 Å, respectively (Figure 1). In addition, there is a distant oxygen (from Gly45) at 2.6 Å and the sulfur of Met121 has moved out to a distance of 3.5 Å, a change of  $\sim 0.4$  Å relative to the native form of the protein. The structure for reduced C112D azurin is unknown. However, the findings that electron self-exchange is  $\sim 10^4$  times slower for C112D azurin than for the WT protein and that electron transfer to a ruthenium-labeled site is at least  $10^3$  times slower suggest that there is a higher Franck–Condon barrier to electron transfer in the mutant protein. This, in turn, implies that the structure of the copper center changes substantially upon reduction.

We have investigated the Cu K edge and EXAFS of C112D azurin. These data indicate that there is both a decrease in covalency and a substantial distortion of the active site upon reduction of this mutant.

- (11) Solomon, E. I.; Baldwin, M. J.; Lowery, M. D. *Chem. Rev.* **1992**, *92*, 521–542.
- (12) Solomon, E. I.; Lowery, M. D. *Science* **1993**, *259*, 1575–1581.
- (13) Lowery, M. D.; Guckert, J. A.; Gebhard, M. S.; Solomon, E. I. *J. Am. Chem. Soc.* **1993**, *115*, 3012–3013.
- (14) Chang, T. K.; Iverson, S. A.; Rodrigues, C. G.; Kiser, C. N.; Lew, A. Y. C.; Germanas, J. P.; Richards, J. H. *Proc. Natl. Acad. Sci. U.S.A.* **1991**, *88*, 1325–1329.
- (15) Karlsson, B. G.; Aasa, R.; Malmström, B. G.; Lundberg, L. G. *FEBS Lett.* **1989**, *253*, 99–102.
- (16) Karlsson, B. G.; Nordling, M.; Pascher, T.; Tsai, L. C.; Sjölin, L.; Lundberg, L. G. *Protein Eng.* **1991**, *4*, 343–349.
- (17) Germanas, J. P.; DiBilio, A. J.; Gray, H. B.; Richards, J. H. *Biochemistry* **1993**, *32*, 7698–7702.
- (18) den Blaauwen, T.; van de Kamp, M.; Canters, G. W. *J. Am. Chem. Soc.* **1993**, *115*, 1121–1129.
- (19) den Blaauwen, T.; van de Kamp, M.; Canters, G. W. *J. Am. Chem. Soc.* **1991**, *113*, 5050–5052.
- (20) Faham, S.; Mizoguchi, T. J.; Adman, E. T.; Gray, H. B.; Richards, J. H.; Rees, D. C. *J. Biol. Inorg. Chem.* **1997**, *2*, 464–469.

- (21) Baker, E. N. *J. Mol. Biol.* **1988**, *203*, 1071–1095.
- (22) Shepard, W. E. B.; Anderson, B. F.; Lewandoski, D. A.; Norris, G. E.; Baker, E. N. *J. Am. Chem. Soc.* **1990**, *112*, 7817–7819.
- (23) Freeman, H. C. *Metalloprotein Crystallography*. In *Spectroscopic Methods in Bioinorganic Chemistry*; ACS Symposium Series 692; Solomon, E. I., Hodgson, K. O., Eds.; American Chemical Society: Washington, DC, 1997; pp 62–95.

## Experimental Section

**A. C112D Azurin Preparation.** *P. aeruginosa* C112D azurin was prepared as described previously.<sup>2,20,24,25</sup> Oxidized C112D azurin was prepared by addition of a slight excess of aqueous CuSO<sub>4</sub> to prepurified apo C112D azurin, followed by treatment with 1 mM EDTA, and purification by cation-exchange chromatography (FPLC (Pharmacia), Mono Q, NaCl gradient in 10 mM diethanolamine, pH = 8.8). The protein concentrations were determined using  $\epsilon_{276} = 2.0 \times 10^3 \text{ M}^{-1} \text{ cm}^{-1}$  and  $\epsilon_{310} = 2.0 \times 10^3 \text{ M}^{-1} \text{ cm}^{-1}$ .<sup>2</sup> The resulting sample was concentrated using Centricon-10. Reduced C112D azurin was prepared by treatment of the oxidized protein with excess dithionite. The excess dithionite was removed, and the buffer changed to 100 mM sodium phosphate (pH = 7.2) by gel filtration through a PD10 column. The protein was concentrated using a Centricon-10. For all XAS samples, glycerol (38%) was added as a glassing agent. Final protein concentrations were all 3.6–4.5 mM. The samples (ca. 120  $\mu\text{L}$ ) were loaded into 1 mm Lucite XAS cells with 63.5 mm Mylar windows and frozen by immersion in liquid nitrogen.

**B. XAS Data Collection and Reduction.** XAS data for oxidized and reduced C112D azurin were measured at the Stanford Synchrotron Radiation Laboratory (SSRL) on unfocused 8-pole wiggler beamline 7–3 under ring conditions 3.0 GeV and 60–100 mA. A Si(220) double-crystal monochromator was utilized for energy selection at the Cu K-edge. The monochromator was detuned 50% to minimize higher harmonic components in the X-ray beam. The samples were maintained at 10 K during the data collection using an Oxford Instruments CF1208 continuous flow liquid helium cryostat. Data were measured in fluorescence mode using a Canberra Ge 13-element array detector. The XAS data were measured to  $k = 15 \text{ \AA}^{-1}$  and  $k = 16 \text{ \AA}^{-1}$  for the oxidized and reduced samples, respectively. Internal energy calibration was performed by simultaneous measurement of the absorption of a Cu foil placed between a second and a third ion chamber. The first inflection point of the Cu foil spectrum was assigned to 8980.3 eV.

The oxidized C112D azurin sample was monitored for photoreduction throughout the course of data collection. A gradual increase in the intensity of the preedge feature at 8984 eV is indicative of photoreduction from Cu(II) to Cu(I).<sup>26</sup> A trend in photoreduction was observed, which resulted in an increase in the intensity of this feature as well as a shift in the edge energy of  $\sim 1.5$  eV between the first and fourth scans and a shift of  $\sim 2$  eV between the first and sixth scans. Analysis of the EXAFS showed less dramatic effects from photoreduction. Two distinct and physically separate spots on the frozen sample were exposed. An average of the first five scans at each spot resulted in very slight differences in the EXAFS at high  $k$ . However, successive two-scan averages from each of the two spots produce nearly identical EXAFS up through the fourth scan. In addition, fits to an average which included only the first scan at each spot produced identical results to an average which included four scans at each spot. Hence, it was determined that the first four scans at each of two spots could be included in the final average for EXAFS fits. (Note that an average including the first scan at each spot is shown for the edge comparison.)

The averaged data for both oxidized and reduced C112D azurin were processed as described previously<sup>27</sup> by fitting a second-order polynomial to the postedge region and subtracting this background from the entire spectrum. A three-region cubic spline was used to model the smooth background above the edge. Normalization of the data was achieved by subtracting the spline and normalizing the edge jump to 1.0 at 9000 eV. Data were converted from energy space to  $k$  space using the equation  $k = [2m_e(E - E_0)/\hbar]^2$ .  $E_0$ , which is defined as the origin of the continuum (the point at which  $k = 0 \text{ \AA}^{-1}$ ), was set at 9000 eV for copper. The resultant EXAFS was  $k^3$ -weighted to enhance the impact of high  $k$  data.

The edge of reduced C112D azurin was analyzed as described previously<sup>26</sup> by a difference comparison with the edges of 2-, 3-, and 4-coordinate Cu(I) model complexes. When the normalized edge of a Cu(II) complex is subtracted from that of a normalized edge of a Cu(I) complex (i.e., reduced C112D azurin), a characteristic derivative shape signal is produced, which can be correlated by shape and energy to the geometry of the copper site.

The EXAFS data analyses were performed using nonlinear least-squares curve-fitting techniques.<sup>28–30</sup> The following models were used to obtain empirical phase and amplitude parameters: Cu–N from Cu(imidazole)<sub>4</sub>(NO<sub>3</sub>)<sub>2</sub>, Cu–O from Cu(acetylacetonate)<sub>2</sub>, and Cu–S from Cu[(C<sub>2</sub>H<sub>5</sub>)<sub>2</sub>(NCS)<sub>2</sub>]<sub>2</sub>. The Fourier transforms (FT) of the EXAFS data were calculated over the ranges  $k = 3.5–15.0 \text{ \AA}^{-1}$  (oxidized) and  $k = 3.5–16.0 \text{ \AA}^{-1}$  (reduced), with a Gaussian window of  $0.1 \text{ \AA}^{-1}$ . The data were then backtransformed with a Fourier filtering window centered on the peak of interest (see Results and Analysis). Curve fitting was performed by varying the structure-dependent parameters. Either coordination number (CN) and distance ( $R$ ) were varied with a fixed Debye–Waller (DW) factor or  $R$  and the DW factor were varied with fixed CN. The DW factor ( $\sigma_{\text{as}}^2$ ) directly relates to the amplitude parameter  $c_2$  in the EXAFS equation,<sup>31</sup> where  $\Delta c_2 = -2\Delta\sigma_{\text{as}}^2$ . A more negative value of  $c_2$  denotes a weaker bond or a greater distribution of scatterers. Conversely, a less negative value of  $c_2$  denotes a stiffer bond or a narrow distribution of scatterers. The importance of the interpretation of  $c_2$  values to EXAFS fit results will be discussed further in Results and Analysis. Note that first shell fits were also performed using FEFF (Version 6.0)<sup>32,33</sup> and produced results that were, within error, identical to those obtained using empirical parameters.

## Results and Analysis

**A. Copper K-Edges.** The X-ray absorption edge of oxidized C112D azurin is characteristic of Cu(II), exhibiting no peak maximum below 8985.0 eV, except for a weak  $1s \rightarrow 3d$  transition at  $\sim 8979$  eV (Figure 2a). The  $1s \rightarrow 4p$  + ligand-to-metal charge transfer (LMCT) shakedown transition of the oxidized mutant is  $\sim 3$  eV higher in energy relative to that of the oxidized form of *P. aeruginosa* azurin<sup>34</sup> (Figure 2b). The process of excitation of a  $1s$  core electron into the  $4p$  orbital (an electron dipole-allowed transition) creates a core hole, which results in an increased effective nuclear charge felt by the valence orbitals. This causes relaxation of the copper valence orbitals to deeper binding energies.<sup>10</sup> The Cu  $3d_{x^2-y^2}$  orbital relaxes to an energy below that of the ligand valence levels. This relaxation allows for a lower energy configuration in which an electron from the ligand valence shell is transferred to fill the Cu  $3d_{x^2-y^2}$  orbital. The more covalent the metal–ligand bond the closer the energy of the ligand  $3p$  is to the Cu  $3d_{x^2-y^2}$  orbital in the ground state. This results in a decrease in the LMCT energy, hence the energy of the shakedown transition decreases as covalency increases. Replacement of the cysteine sulfur by the less covalent oxygen of aspartate in C112D azurin results in an increase in the energy of the shakedown transition.

Reduced C112D azurin shows a distinctive shoulder at 8984 eV characteristic of Cu(I). By comparing the intensity of the 8984 eV transition of reduced C112D azurin to that in edges of

- (24) Mizoguchi, T. J.; Di Bilio, A. J.; Gray, H. B.; Richards, J. H. *J. Am. Chem. Soc.* **1992**, *114*, 10076–10078.  
 (25) Piccioli, M.; Luchinat, C.; Mizoguchi, T. J.; Ramirez, B. E.; Gray, H. B.; Richards, J. H. *Inorg. Chem.* **1995**, *34*, 737–742.  
 (26) Kau, L. S.; Spira-Solomon, D. J.; Penner-Hahn, J. E.; Hodgson, K. O.; Solomon, E. I. *J. Am. Chem. Soc.* **1987**, *109*, 6433–6442.  
 (27) DeWitt, J. G.; Bentsen, J. G.; Rosenzweig, A. C.; Hedman, B.; Green, J.; Pilkington, S.; Papaefthymiou, G. C.; Dalton, H.; Hodgson, K. O.; Lippard, S. J. *J. Am. Chem. Soc.* **1991**, *113*, 9219–9235.

- (28) Cramer, S. P.; Hodgson, K. O.; Stiefel, E. I.; Newton, W. E. *J. Am. Chem. Soc.* **1978**, *100*, 2748–2761.  
 (29) Cramer, S. P.; Hodgson, K. O. *Prog. Inorg. Chem.* **1979**, *25*, 1–39.  
 (30) Scott, R. A. *Methods Enzymol.* **1985**, *117*, 414–440.  
 (31) Stern, E. A. *X-ray Absorption: Principles, Applications, Techniques of EXAFS, SEXAFS, and XANES*; Koningsberger, D. C., Prins, R., Eds.; John Wiley and Sons: New York, 1988; Vol. 92, pp 3–51.  
 (32) Rehr, J. J.; Mustre de Leon, J.; Zabinsky, S. I.; Albers, R. C. *J. Am. Chem. Soc.* **1991**, *113*, 5135–5140.  
 (33) Mustre de Leon, J.; Rehr, J. J.; Zabinsky, S. I.; Albers, R. C. *Phys. Rev.* **1991**, *B44*, 4146–4156.  
 (34) Oxidized azurin samples were 4.0 mM in copper, pH = 7.0 in 50 mM phosphate buffer. The data for WT azurin were collected under the same conditions as those employed for C112D azurin samples.

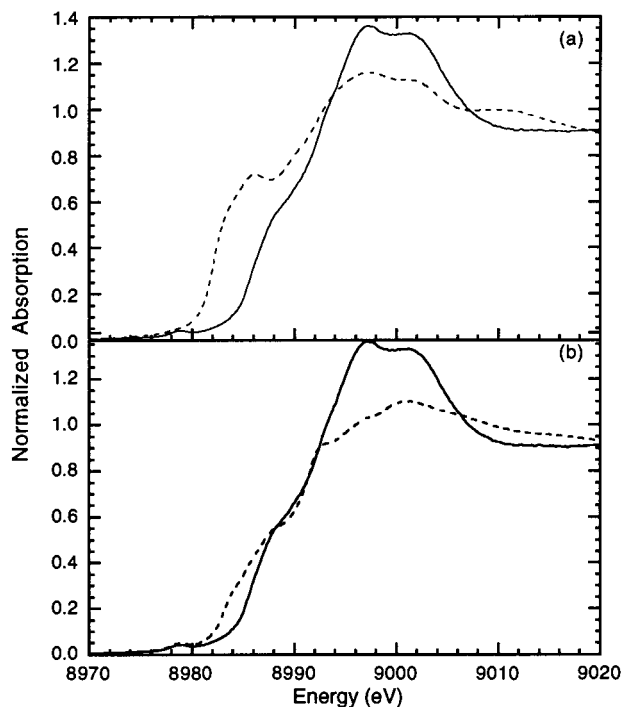


**Figure 2.** (a) Comparison of the normalized Cu K-edge XAS spectra of oxidized (—) and reduced (---) forms of C112D azurin. (b) Comparison of the normalized Cu K-edge XAS spectra of oxidized C112D azurin (—) and oxidized azurin<sup>34</sup> (---).

copper complexes of known coordination, it appears that the mutant contains either 3- or 4-coordinate copper. Two-coordinate Cu(I) complexes exhibit a sharp, intense preedge absorption peak in the 8984 eV region.<sup>26</sup> When the coordination number of the copper site is increased, the intensity of this feature decreases as a result of a change in the ligand field splitting of the copper 4p orbitals. A difference edge analysis allows the changes in the 8984 eV peak intensity, which result from changes in active site geometry, to be quantified. The difference spectra of 3-coordinate Cu(I) complexes have a positive peak at 8983.1–8983.8 eV, while 4-coordinate Cu(I) complexes have a peak in the 8984.7–8986.3 eV region. An edge difference analysis was performed by subtracting the normalized edge of a Cu(II) complex (created by averaging a group of “noncovalent”<sup>35</sup> model complexes in order to produce an essentially featureless edge) from that of reduced C112D azurin. This results in a signal which most closely resembles a 3-coordinate complex in energy, shape, and intensity, as seen in Figure 3. Although the energy of the positive peak in the difference spectra of reduced C112D azurin is slightly higher in energy (8984.1 eV) than the range seen for 3-coordinate models,<sup>26</sup> the difference spectrum is clearly closer to a 3-coordinate than to a 4-coordinate system. This is reasonable for a mutant in which the blue copper center has been destroyed, as normal Cu(I) prefers either linear or trigonal coordination.<sup>36,37</sup>

**B. EXAFS.** The EXAFS data for oxidized and reduced forms of C112D azurin were Fourier transformed over the ranges  $k = 3.5\text{--}15.0 \text{ \AA}^{-1}$  and  $k = 3.5\text{--}16.0 \text{ \AA}^{-1}$ , respectively (data

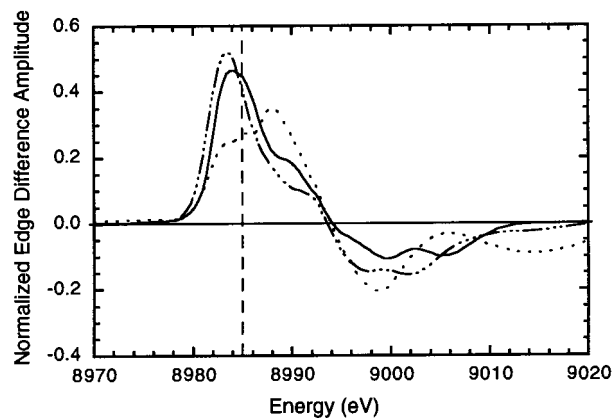


**Figure 3.** Normalized edge difference spectra of reduced C112D azurin (—) and representative 3- (····) and 4-coordinate models (---). The vertical line indicates 8985.0 eV.

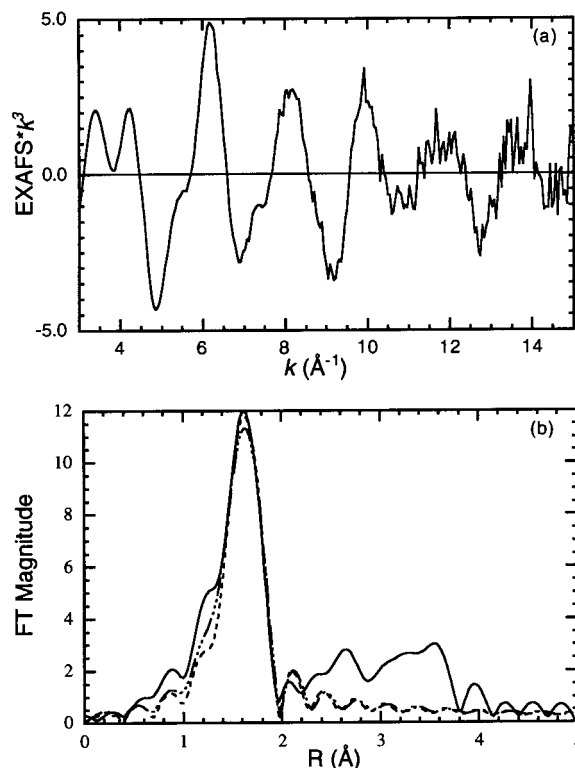


**Figure 4.** (a) EXAFS spectrum of oxidized C112D azurin. (b) The nonphase shift-corrected Fourier transform of the EXAFS (—); FT for the best one-wave (---) and two-wave (····) fits.

shown in Figures 4a and 5a). The first coordination shell data were backtransformed with corresponding Fourier transform windows of 0.9–2.1 and 0.9–2.2 Å and then fit over the ranges  $k = 3.75\text{--}14.75 \text{ \AA}^{-1}$  and  $k = 3.75\text{--}15.75 \text{ \AA}^{-1}$ , for the oxidized and reduced forms, respectively (Fourier transforms shown in Figures 4b and 5b).

The best single wave fit of oxidized C112D azurin was obtained by positioning 3.2 nitrogens at a distance of 2.01 Å (Figure 4b, Table 1). As indicated in Table 1, two-wave fits, where a contribution at a longer or a shorter Cu–N distance was included, did not show a significant improvement in the F (goodness of fit) value. By allowing  $c_2$  and  $R$  to vary while stepping through fixed coordination numbers, essentially identical results were obtained for the single-wave fit, showing 3.2–3.4 N’s at a distance of 2.01 Å. If a second longer Cu–N interaction was included, the  $c_2$  parameter from the model compounds would be slightly too small to compensate for this

(35) The following compounds were used:  $\text{Cu}(\text{ImH})_4(\text{NO}_3)_2$ ,  $\text{Cu}[\text{2-hydroxyacetophenimino}]_2\text{en}[\text{CuCl}_2]$ , and  $\{\text{Cu}_2[\text{2-hydroxy-1,3-propylenediamine-}N,N,N',N'\text{-tetrakis}(N\text{-ethylbenzimidazol-2-yl})](\text{OAc})\}\text{-ClO}_4$ .

(36) Kitajima, N.; Fujisawa, K.; Moro-oka, Y. *J. Am. Chem. Soc.* **1990**, *112*, 3210–3212.

(37) Jameson, G. B.; Ibers, J. A. *Bioinorganic Chemistry*; Bertini, I., Gray, H. B., Lippard, S. J., Valentine, J. S., Eds.; University Science Books: Mill Valley, CA, 1994; pp 167–252.

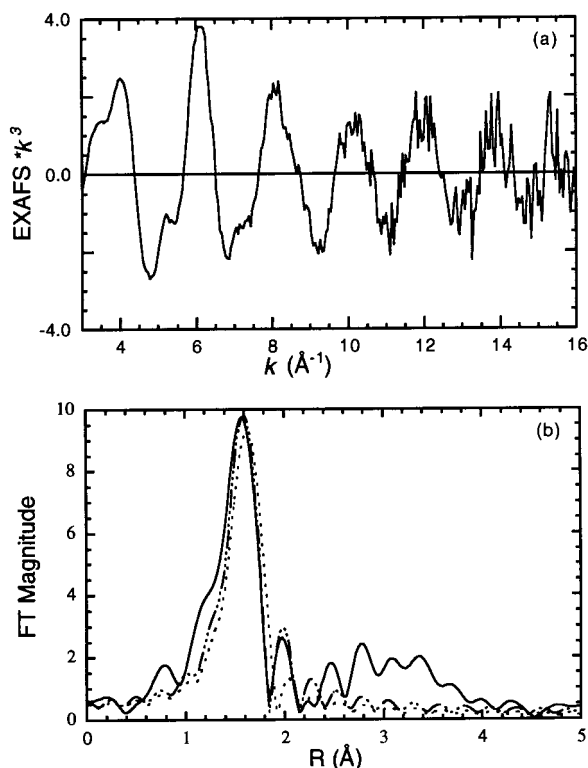


**Figure 5.** (a) EXAFS spectrum of reduced C112D azurin. (b) The nonphase shift-corrected Fourier transform of the EXAFS (—); the FT for the best one- (---) and two-wave (-·-·-) fits.

**Table 1.** Results of Least-Squares Refinement Fits for Oxidized C112D Azurin<sup>a</sup>

fit no. <sup>b</sup>	element	CN	<i>R</i> (Å)	<i>F</i> <sup>c</sup>	<i>c</i> <sub>2</sub> (Å <sup>2</sup> )
<i>R</i> and CN Varied, <i>c</i> <sub>2</sub> Fixed at -0.016 and -0.017 Å <sup>2</sup> for N and O, Respectively					
1	N	3.2	2.01	0.29	
2	N	3.2	2.00		
	N	0.21	2.38	0.27	
3	N	2.9	2.01		
	N	0.55	1.95	0.27	
4	O	2.8	1.98	0.25	
5	O	3.0	1.98		
	O	0.33	1.82	0.23	
6	N	3.3	2.00		
	O	0.10	2.92	0.23	
<i>R</i> and <i>c</i> <sub>2</sub> Varied, CN Stepped through Fixed Values at Intervals of 0.1–0.5					
1	N	4.5	2.01	0.38	-0.016
2	N	4.0	2.01	0.31	-0.014
3	N	3.5	2.01	0.28	-0.013
4	N	3.4	2.01	0.28	-0.013
5	N	3.3	2.01	0.28	-0.013
6	N	3.2	2.01	0.28	-0.011
7	N	3.0	2.01	0.30	-0.011
8	N	2.5	2.01	0.39	-0.010
9	N	2.0	2.01	0.52	-0.008
10	N	3.4	2.01		-0.013
	N	0.5	2.35	0.26	-0.027
11	N	3.4	2.01		-0.013
	N	1.0	2.32	0.26	-0.051

<sup>a</sup> Errors are estimated to be 0.02–0.03 Å for distances and 25% for coordination numbers.<sup>28</sup> <sup>b</sup> All fits were performed using an FT window of 0.9–2.1 Å. <sup>c</sup> The *F* value is a measure of the goodness of fit, which is defined as,  $F = [(\sum_i [k^3(\text{EXAFS}_{\text{obs}} - \text{EXAFS}_{\text{calc}})_i])^2/n]^{1/2}$ , where *n* = the number of data points *i*.

longer bond and hence could result in an underestimated CN. This possibility was tested by allowing *c*<sub>2</sub> and *R* to vary while holding CN at fixed values. As indicated by the results

**Table 2.** Results of Least-Squares Refinement Fits for Reduced C112D Azurin<sup>a</sup>

fit no.	element	CN	<i>R</i> (Å)	<i>F</i>	<i>c</i> <sub>2</sub> (Å <sup>2</sup> )
<i>R</i> and CN Varied, <i>c</i> <sub>2</sub> Fixed at -0.016 and -0.009 Å <sup>2</sup> for N and S, respectively <sup>b</sup>					
1	N	2.3	2.00	0.40	
2	N	2.6	1.99		
	N	0.72	2.14	0.30	
3	N	2.3	2.00	0.39	
4	N	2.8	1.99		
	N	0.98	2.17	0.26	
5	N	2.7	1.99		
	N	0.85	2.13		
	S	0.21	2.43	0.27	
6	N	2.6	1.99		
	N	0.72	2.14		
	S	0.06	3.18	0.29	
<i>R</i> and <i>c</i> <sub>2</sub> Varied, CN Stepped through Fixed Values at Intervals of 0.1–0.5 <sup>c</sup>					
1	N	4.0	2.00	0.53	-0.019
2	N	3.0	2.00	0.45	-0.015
3	N	2.5	2.00	0.43	-0.013
4	N	2.0	2.00	0.45	-0.011
5	N	1.5	2.00	0.53	-0.011
6	N	2.0	1.98		-0.009
	N	1.0	2.12	0.30	-0.017
7	N	2.0	1.98		-0.010
	N	2.0	2.11	0.26	-0.028
8	N	3.0	2.00		-0.013
	N	1.0	2.18	0.26	-0.013

<sup>a</sup> Errors are estimated to be 0.02–0.03 Å for distances and 25% for coordination numbers.<sup>28</sup> <sup>b</sup> Fits 1, 2, 5, and 6 were performed using an FT window of 0.9–1.9 Å; fits 3 and 4 were performed using an FT window of 0.9–2.2 Å. <sup>c</sup> All fits were performed using an FT window of 0.9–2.2 Å.

summarized in Table 1, a second-wave fit with a coordination number of one results in unrealistically high values for *c*<sub>2</sub> and still shows no significant improvement in the *F* value relative to the single-wave fit. Fits were also performed using Cu–O model parameters or a combination of Cu–O and Cu–N model parameters. The fit results are essentially the same as those obtained by using only Cu–N waves (Table 1). This is expected, as one of the limitations of the EXAFS technique is its inability to distinguish between atoms adjacent in the periodic table (i.e., C, N, O) due to their similar backscattering properties.

The data for reduced C112D azurin (Figure 5) were fit using both a narrow and wide Fourier backtransform window to include a feature at ~2.0 Å. The best fit results using a narrow window show 2.3 N's at a distance of 2.00 Å, with an *F* value of 0.40. The single wave fit clearly showed a mismatch of phase in *k* space, as well as a mismatch in phase and intensity in *R* space. The addition of a second Cu–N wave results in a fit of 2.6 N's at 1.99 Å and 0.72 N's at 2.14 Å, with an *F* value of 0.30, indicating a significant improvement in the goodness of fit. This is clearly seen in Figure 5b, which shows an improvement in *R* space in the two-shell fits. The best one-wave fit for the reduced C112D azurin using a wide Fourier transform window shows 2.3 N's at a distance of 2.00 Å, with an *F* value of 0.39. The two-wave fit over this region shows 2.8 N's at 1.99 Å and 0.98 N's at 2.17 Å, with an *F* value of 0.26. Once again, the addition of a second wave showed significant improvement in the fit for reduced C112D azurin (see Figure 5b, Table 2). Finally, a third wave of Cu–S backscattering was tested. The fits did not improve the *F* value and resulted in unreasonable values for the number of coordinating sulfurs. The results from the fits in which *c*<sub>2</sub> and *R* were allowed to vary while stepping through fixed coordination numbers indicate that the above values do represent the best fit, as well as the most

reasonable values for  $c_2$ . An artificially high coordination number for the second wave results in the  $c_2$  value becoming unreasonably large (Table 2).

### Discussion

The XAS data for oxidized C112D azurin are in agreement with crystallographic results.<sup>20</sup> The three N/O waves at  $\sim 2.0$  Å correspond to the average distance of the 1.9 Å Cu–O bond to Asp112, the 2.0 Å Cu–N bond to His46, and the 2.1 Å Cu–N bond to His117. We would not expect to observe the longer oxygen distances ( $\sim 2.5$ – $2.6$  Å) by EXAFS, since both oxygen and nitrogen are relatively weak backscatterers, and at the long distance indicated by crystallography would be only weakly coordinated and accordingly would exhibit high thermal motion. The edge of oxidized C112D azurin indicates a significant decrease in covalency relative to the oxidized edge of WT azurin. In order for the metal center to couple into electron-transfer pathways there must be covalency in the metal–ligand bond.<sup>38</sup> A bond with higher covalency (stronger coupling) will mediate electron transfer more efficiently (rate is proportional to the square of the coupling). Hence, the decrease in covalency in C112D azurin indicates one contribution to the decrease in electron-transfer rates.

The EXAFS data for reduced C112D azurin show two or three N/O's at 1.99 Å and one N/O at 2.17 Å. The edge difference analysis indicates that the structure is approximately 3-coordinate, which is common for Cu(I).<sup>36,37</sup> Assignment of

ligands is aided by computer modeling studies which suggest that in the reduced form the aspartate carboxylate is either monodentate or is completely detached.<sup>2</sup> If aspartate is monodentate, there would be an increase in the Cu–O distance in an active site structure in which the Cu–N bonds to the imidazole would not be perturbed significantly. Alternatively, if the Asp carboxylate were completely detached, the oxygen atom of the Gly45 carbonyl could move closer to the reduced Cu center, producing a 3-coordinate structure. In either case, a  $\sim 0.2$  Å distortion occurs upon reduction, in which the active site undergoes a slight expansion within the trigonal plane. When compared to the findings for *A. denitrificans* azurin, where essentially no change is observed within the trigonal plane upon reduction, the distortion in the C112D azurin mutant appears significant. The larger distortion of the copper site in the C112D mutant implies a larger Franck–Condon barrier to electron transfer, and suggests a second contribution to the relatively slow electron-transfer rates of the mutant as compared to native azurin.

**Acknowledgment.** This research was supported by the NSF [CHE-9217628 (E.I.S.); CHE-9423181 (K.O.H.)] and the NIH [RR-01209 (K.O.H.); DK-19038 (H.B.G.)]. SSRL operations are funded by the Department of Energy, Office of Basic Energy Sciences. The Biotechnology Program is supported by the National Institutes of Health, National Center for Research Resources, Biomedical Technology Program and by the Department of Energy, Office of Biological and Environmental Research.

IC9804622

(38) Holm, R. H.; Kennepohl, P.; Solomon, E. I. *Chem. Rev.* **1996**, *96*, 2239–2314.